

Coupled 2-D and 3-D modelling of coastal hydrodynamics

Modèle
Bidimensionnel
Tridimensionnel
Loire
Vilaine

Model
Two-dimensional
Three-dimensional
Loire
Vilaine

Pascal LAZURE, Jean-Claude SALOMON

Institut Français de Recherche pour l'Exploitation de la Mer (IFREMER), Centre de Brest, B.P. 70, 29280 Plouzané.

Received 5/02/90, in revised form 1/06/90, accepted 31/07/90.

ABSTRACT

The hydrodynamics of coastal zones often reflect the combined action of tides, winds and density differences. Usual two-dimensional numerical models are only partly suited to the study of such mechanisms.

A set of two 2-D and 3-D numerical models is described here. Its main characteristics are: an automatic coupling, a specific procedure for shoaling banks, a reduced vertical coordinate system, and a resolution by finite differences.

As an example, the complete set is applied to the region of the Loire and Vilaine estuaries in South Brittany (France). Results prove to be coherent with experimental data and enhance our knowledge of the local hydrodynamics.

Oceanologica Acta, 1991, 14, 2, 173-180.

RÉSUMÉ

Modélisation de l'hydrodynamique côtière par des modèles 2D et 3D couplés

L'hydrodynamique des zones côtières est souvent due aux actions combinées de la marée, du vent et des écarts de densités, mécanismes pour lesquels les modèles bidimensionnels habituels s'avèrent peu adaptés.

On décrit ici un ensemble couplé de modèles à deux et à trois dimensions spatiales. Les caractéristiques principales sont : une procédure de couplage automatique, la prise en compte des zones découvrantes, un système de coordonnées verticales réduites et une méthode de résolution en différences finies.

A titre d'exemple, le modèle complet est appliqué à la zone des estuaires de la Loire et de la Vilaine. Les résultats s'avèrent conformes aux faits expérimentaux et accroissent notre connaissance de l'hydrodynamique locale.

Oceanologica Acta, 1991, 14, 2, 173-180.

INTRODUCTION

There is an increasing need to understand the dynamics of coastal and littoral zones because of its important influence on sedimentary, chemical and biological processes. For many years, mathematical models have demonstrated

constantly increasing efficiency; they are now necessary tools for any multidisciplinary team working in the domain of coastal studies.

The object of the present paper is to present two models developed at IFREMER, together with a practical example of application to a local study. The first model is two-

dimensional and benefits from all the experience gained with this kind of model during the last fifteen years. The automation of several tasks in its use makes it a very efficient and easy to use system. However, this type of model has its limitations, and proves inadequate when dynamics becomes three-dimensional, as in the case of wind circulation or river plumes. A 3-D model has recently been developed to describe a large range of physical processes. The two models together form a coherent system which permits a 3-D calculation, longer and therefore more costly, in areas where this is absolutely necessary.

THE TWO-DIMENSIONAL MODEL

Equations

With the very classical Boussinesq and hydrostatic pressure hypotheses, one obtains the Saint-Venant equations by integrating the Navier-Stokes equations in the case of an homogeneous ocean:

$$\frac{\partial U}{\partial t} + U \frac{\partial U}{\partial x} + V \frac{\partial U}{\partial y} - fV = -g \frac{\partial \zeta}{\partial x} + N_H \nabla_H^2 U + (\tau_{xs} - \tau_{xb}) / \rho_0 D \quad (1)$$

$$\frac{\partial V}{\partial t} + U \frac{\partial V}{\partial x} + V \frac{\partial V}{\partial y} + fU = -g \frac{\partial \zeta}{\partial y} + N_H \nabla_H^2 V + (\tau_{ys} - \tau_{yb}) / \rho_0 D \quad (2)$$

The integration of the continuity equation yields :

$$\frac{\partial \zeta}{\partial t} + \partial (DU) / \partial x + \partial (DV) / \partial y = 0 \quad (3)$$

where ζ : elevation of free surface; D : water depth; (U, V) : components of average velocity; τ_s : surface friction; τ_b : bottom friction; f : Coriolis coefficient; g : acceleration of gravity; ρ_0 : reference density; and N_H : coefficient of turbulent horizontal viscosity.

Surface and bottom friction are parametrized :

$$(\tau_{xs}, \tau_{ys}) = \rho_a C_{da} \sqrt{U_w^2 + V_w^2} (U_w, V_w) \quad (4)$$

$$(\tau_{xb}, \tau_{yb}) = g \sqrt{U^2 + V^2} / K_r D^{1/3} (U, V) \quad (5)$$

where ρ_a : air density; C_{da} : drag coefficient; (U_w, V_w) components of wind velocity; and K_r : Strickler coefficient.

Numerical method of integration

The numerical integration method is of ADI type (Peaceman and Rachford, 1955). The critical time step, estimated by extracting from the equations only the acceleration and bottom friction terms, follows the relation :

$$\Delta t < 3 \cdot 10^{-3} \Delta x^2 / D |U|.$$

Spatial discretization of equations 1 to 3 is done according to a "C" type grid, slightly modified for what concerns water depths which are indicated at the same location as velocity components.

An automatic treatment of emerging tidal flats has been introduced as follows: in an ADI procedure, the equation of motion ($n^{\circ}1$) at time level t is transformed into a relation of the form:

$$-\alpha \zeta_{x+\Delta x/2}^{t+\Delta t} + \beta U_x^{t+\Delta t} + \alpha \zeta_{x+\Delta x/2}^{t+\Delta t} = \gamma$$

where α , β and γ are known quantities which only depend on variables U , V and ζ at previous time steps t and $t - \Delta t$. In the case of emerging zones (surface elevation inferior or equal to bottom height), a test is made which imposes $\alpha = 0$ and $\gamma = 0$.

This clearly makes the velocity U be zero, while preserving the linear form of the relation. The usual matrix resolution is then made for the whole domain, irrespective of the existence of permanent or occasional land barriers.

Boundary conditions

The boundary conditions for velocities at the coast is simply written by imposing a zero flux across the coastline.

On the open boundaries, elevations and one current component must be specified at each grid point. However, in practice, the setting of levels linked only to a condition of radiation on velocities is sufficient to pilot the model.

A problem emerges with the usually unknown levels on the boundaries. The present model is considered as a sub-model operating inside a larger one, for which boundary conditions are interpolated among the few available measurements at sea, and for which a coarser mesh is acceptable.

Calculated elevations along the frontiers of the subdomain are then stored and used later as boundary conditions for the model of limited extent.

The procedure may be repeated if necessary, restraining on each occasion the domain, the grid size and the time step.

In the present model, this method has been automatized. The programme performs by itself the different interpolations in space and time needed for extracting the water levels from results of the preceding model and constructing the adequate numerical grid.

This imbrication system permits to correctly simulate of tide propagation on the shelf and mean level variations due to wind.

THE THREE-DIMENSIONAL MODEL

Equations

The 3-D model solves the complete set of Navier-Stokes equations simplified by the Boussinesq hypothesis and by a pressure-assumed hydrostatic. Instead of directly addressing volumetric masses, equations have been modified to include a buoyancy parameter.

$$b = g (\rho_o - \rho) / \rho_o.$$

In order to maintain a constant number of grid points on the water column during the vertical discretization, a change of coordinate system is done:

$$(x, y, z, t) \rightarrow (x, y, \sigma, t) \text{ where } \sigma = (\zeta + H) / D.$$

Equations in this new system become:

$$\begin{aligned} \partial u / \partial t + u \partial u / \partial x + v \partial u / \partial y + \omega^* \partial u / \partial \sigma - f v \\ = - \partial p / \partial x + (1/D^2) \partial / \partial \sigma [N_z \partial u / \partial \sigma] + F_x \end{aligned} \quad (7)$$

$$\begin{aligned} \partial v / \partial t + u \partial v / \partial x + v \partial v / \partial y + \omega^* \partial v / \partial \sigma + f u \\ = - \partial p / \partial y + (1/D^2) \partial / \partial \sigma [N_z \partial v / \partial \sigma] + F_y \end{aligned} \quad (8)$$

$$p = g \zeta + D \int_{\sigma}^1 b \, d\sigma. \quad (9)$$

Continuity equation

$$\partial \zeta / \partial t + \partial u / \partial x + \partial v / \partial y + D \partial \omega^* / \partial \sigma = 0 \quad (10)$$

where

$$\begin{aligned} \omega = D \omega^* + \sigma \partial \zeta / \partial t - U [\partial H / \partial x - \sigma \partial D / \partial x] \\ - V [\partial H / \partial y - \sigma \partial D / \partial y] \end{aligned}$$

(u, v, w) : components of velocity in (x, y, z, t) system :

$$H = D - \zeta$$

N_z : vertical eddy viscosity

The transformation of diffusion terms (F_x , F_y) in the new system becoming really complex, those are approximated by :

$$(F_x, F_y) = N_h V_h^2 (u, v)$$

This simplification, commonly applied when using Sigma-coordinates, cannot notably modify the precision of the results since these terms are generally of an order of magnitude lower than the terms of vertical shear.

To the above equations is usually added that of advection dispersion of a substance in solution.

$$\begin{aligned} \partial D c / \partial t + \frac{\partial D (u c - K_x \partial c / \partial x)}{\partial x} + \frac{\partial D (v c - K_y \partial c / \partial y)}{\partial y} \\ + \frac{\partial [D \omega^* c - (K_z / D) (\partial c / \partial \sigma)]}{\partial \sigma} = 0. \end{aligned} \quad (11)$$

Finally, to close up the system when the substance in solution acts on water density, a state equation is necessary. In the case where only salinity variations are considered, this may be approximated by:

$$b = g \cdot 0,76 \cdot (S - S_o) \quad (12)$$

Boundary conditions

At the surface:

$$N_z / D [\partial u / \partial \sigma, \partial v / \partial \sigma]_{\sigma=1} = (\tau_{x_s}, \tau_{y_s})$$

$$\omega^* = 0$$

$$[D \omega^* c - (K_z / D) \cdot (\partial c / \partial \sigma)]_{\sigma=1} = 0 \quad (13)$$

in the case where there is no exchange through the surface

At the bottom:

$$\begin{aligned} N_z / D [\partial u / \partial \sigma, \partial v / \partial \sigma]_{\sigma=0} = (\tau_{x_b}, \tau_{y_b}) \\ = \rho c_d \sqrt{u_b^2 + v_b^2} (u_b, v_b) \end{aligned}$$

$$\omega^* = 0$$

$$[D \omega^* c - (K_z / D) \cdot (\partial c / \partial \sigma)]_{\sigma=0} = 0 \quad (14)$$

Bottom tensions are quadratic functions of velocities at the bottom, and implicitly assume a logarithmic velocity profile near the bottom.

$$C_d = 0.16 [\log z / z_0]^{-2} \quad (15)$$

Z_o = roughness parameter.

Turbulence

In the present version of the model, the coefficient of turbulent exchanges is calculated assuming local equilibrium between production and dissipation of turbulent energy.

$$N_z = D U^* \sigma (1 - \sigma)^{1/2} (1 + 10 R_i)^{-1/2} \quad (16)$$

$$K_z = D U^* \sigma (1 - \sigma)^{1/2} (1 + 3.33 R_i)^{-3/2} \quad (17)$$

$$R_i = D \partial b / \partial \sigma [(\partial u / \partial \sigma)^2 + (\partial v / \partial \sigma)^2]^{-1}$$

The reduction of turbulent exchanges near a strong stratification is taken into account by a parameterization with respect to the Richardson number identical to the Munk and Anderson (1948) formulation.

These two formulations, although they take into account some physical processes, contain an important element of empiricism. They require a comparison between model results and measurements in order to calibrate coefficients where a detailed treatment of turbulence is necessary, as in the case of plume dynamics.

Numerical method of resolution

Principle

The resolution of the equation system (7) - (10) is based on the separation of external and internal modes (Blumberg and Mellor, 1981). The advantage of this method is to allow the three-dimensional calculation of currents to run without the time step limitation imposed for wave propagation.

The two models run in parallel. The 2-D model described above calculates the free surface elevations and yields them to the three-dimensional model. The latter solves the complete equations. Knowledge of the current and density

field makes it possible to introduce into the 2-D model terms depending on an approximation, such as bottom friction, current shear and mean internal pressure gradients.

Numerical scheme

The spatial discretization of equations is done according to the grid described above. Over the vertical, the principle is the same.

The time discretization is of leap-frog type. For stability reasons, two terms are estimated at different times. Terms of horizontal diffusion are calculated at the first time step and terms including vertical derivative are taken implicitly. In order to avoid time-splitting instabilities, the Asselin filter (Asselin, 1972) is applied at each time step.

Coupling

The time step constraint of the 3-D model is linked to the current velocity by $\Delta t < \Delta x / u$. The coupling of the two models is not simple and is rarely evoked. The transmission of the bottom friction term (usually of an order of magnitude greater than the lateral shear terms) calculated

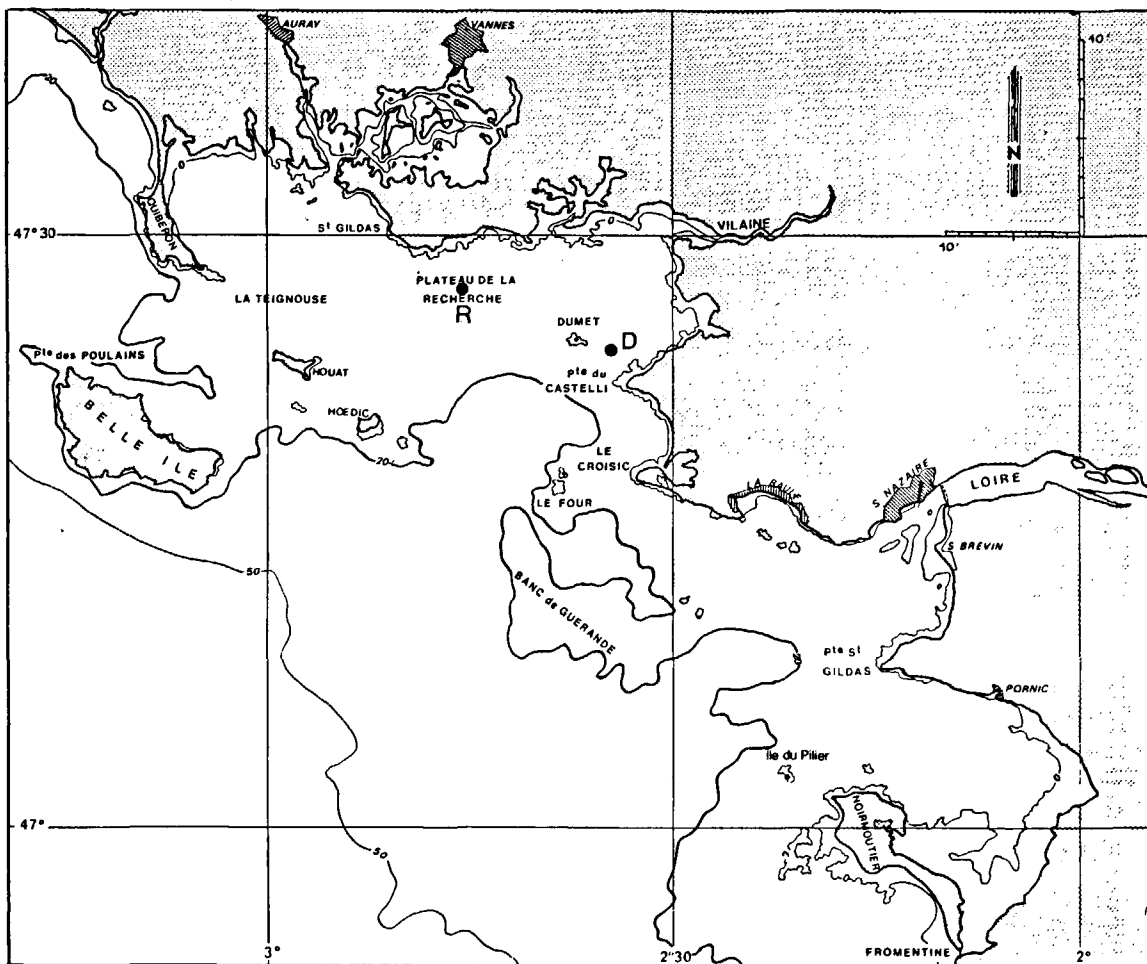


Figure 1

The Mor Bras Zone.
La zone du Mor Bras

by the 3-D model to the 2-D model creates a decrease of stability. In fact, the critical time step of the 2-D model depends on the semi implicit formulation of friction which acts as a stabilizing term.

In order to keep in part the advantages of ADI, the friction term is calculated in a hybrid manner:

$$\tau_{2d} = (\tau_{3d})_{t=t_0} + [(\tau_{2d})_{impl} - (\tau_{2d})_{t=t_0}]$$

τ_{2d} is the bottom stress used by the 2-D model, $\tau_{2d} impl$ is the bottom stress calculated by the 2-D semi-implicit formulation and $(\tau_{3d})_{t=t_0}$, $(\tau_{2d})_{t=t_0}$ are those calculated by the two models before coupling.

The occasional oscillations of leap-frog type resulting from the coupling of the two models and described by Gordon (1982) are dampened by a slight filter over two time steps of friction terms provided to the 2-D model.

It has not yet been possible to define a universal criterion for the 2-D model critical time step and for the maximum ratio between the two time steps.

Advection dispersion model

Solving equation (11) is done with the method of fractional steps. Advection in the horizontal plane is done with the Takacs method (1985) which is a modification of Lax Vendroff scheme to bring it to the third order. For stability reasons, vertical advection terms are considered as semi-implicit with the Euler modified method (Roache, 1982), precise to the second order.

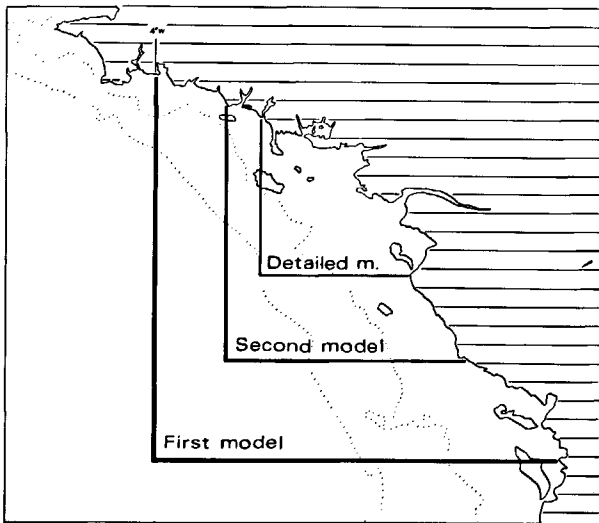


Figure 2

Extension of the three models. Grid size is 6 km for the largest domain and 3 km for the next largest. The smallest, which was used later for the whole study, has a grid size of 1 km for the 2-D computation and 2 km for the coupled 2-D-3-D computation.
 Extension des trois modèles. La maille est de 6 km pour le plus grand domaine et 3 km pour le suivant. Le plus petit ayant été utilisé ensuite pour la totalité de l'étude a une maille de 1 km pour le calcul 2D et de 2 km pour le calcul couplé 2D-3D.

Table

Comparison between computed and calculated current ellipse parameters. a : semi-major axis; b : semi-minor axis; α : orientation of the semi-major axis.

Comparaison entre les paramètres des ellipses de courant calculés et mesurés. a : demi grand axe ; b : demi petit axe ; α : orientation du demi grand axe.

	a _{mes}	a _{comp}	b _{mes}	b _{comp}	α_{mes}	α_{comp}
Point D-surface	33.3	39.7	-7.2	-4.0	46	43.6
Point D-bottom	14.6	12.8	1.7	1.8	47.8	46.8
Point R-surface	13.2	10.4	8.0	5.6	60.1	70.1
Point R-bottom	13.0	8.1	3.5	5.3	60.3	64.3

Boundary conditions

The problem of providing levels on the boundaries does not concern directly the 3-D model and is treated by the 2-D model imbrication method previously described.

Although it is theoretically necessary to provide the vertical velocity profiles on the boundaries, a radiation condition or an Ekman-type relation (Burg *et al.*, 1982) is commonly used due to the lack of data. The latter has been tested but not retained because it can induce instabilities, particularly when the bathymetry is not regular.

Actually, the velocity gradient at each level is set to zero at the boundary. This very simple condition appears satisfactory when the domain is friction-dominated. The fact that this solution may be adequate results in great measure from the imposed levels at the boundary and the dampening of perturbations by friction. No tests have yet been done when density gradients appear at the boundaries, but it may be anticipated that this solution could become unadapted. The question of boundary conditions is still an open one. Rather than to test every published solution (like radiation conditions), whose any is universal, we prefer to extend the imbrication model concept to the 3-D modelization. This work is now in progress.

Introduction of rivers

Considering the functioning mode of the 2-D model, a river is introduced by adding an additional step every 1/2 time step

$$\partial \zeta / \partial t = Q / \Delta x^2$$

Q = river discharge

In nature this is equivalent to adding every 1/2 time step a water amount equal to that brought in by the river during this length of time. For the 3-D model, it is assumed that water is input at the surface, which is equivalent to writing

$$\omega_{\sigma=1}^* = - (Q / D \Delta x^2) \Delta t.$$

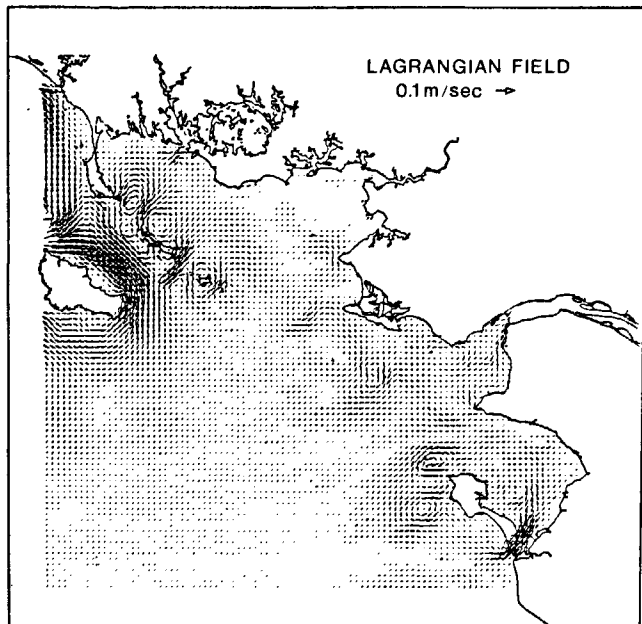


Figure 3
Computed residual Lagrangian currents.
Courants lagrangiens calculés.

This condition, which does not assume any velocity profile in the river, is very satisfactory and permits, when simulating a plume, the introduction of a fresh water amount corresponding to the simulated discharge.

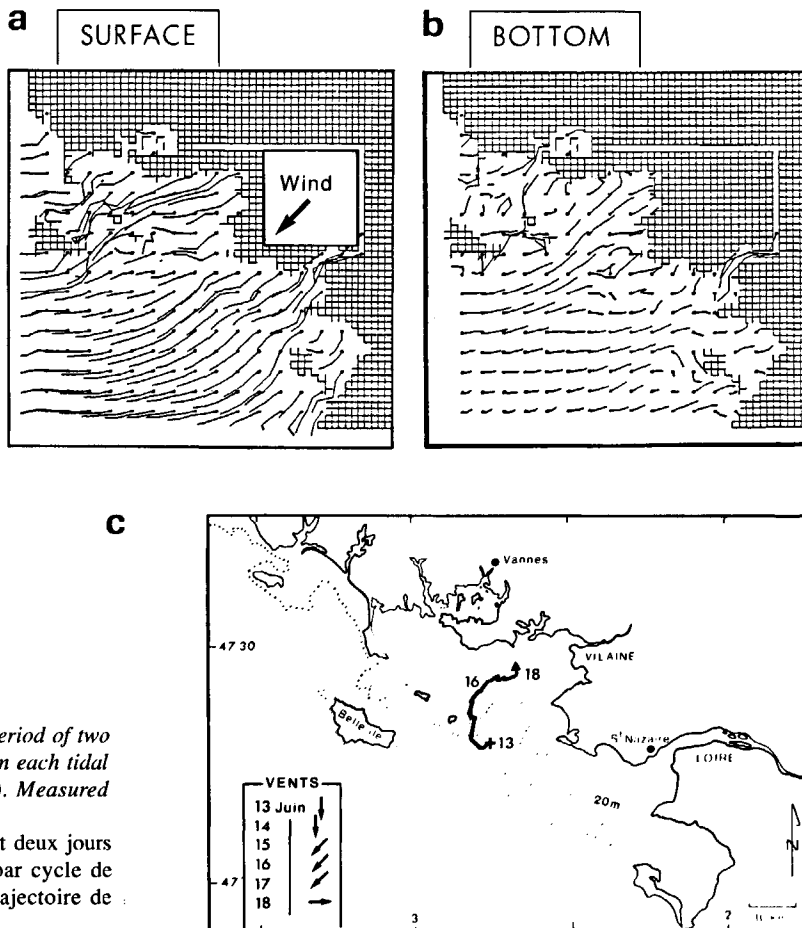
APPLICATION TO THE MOR BRAS ZONE

The studied area is located on the Atlantic coast of France and is characterized by an irregular coastline and a rough bathymetry (Fig. 1). The two river inputs are the Loire and the Vilaine, whose average discharges are 800 m³/s and 80 m³/s respectively.

A detailed study of the area has recently been done with the above two models (Salomon and Lazure, 1988). Three application examples corresponding to each of the main dynamic processes are presented. The time steps used for the 2-D and 3-D models were respectively 120 and 240 seconds

Figure 4

Computed horizontal and vertical trajectories over a period of two days (the tide is filtered out by reporting one point from each tidal cycle). Near the surface (a) and near the bottom (b). Measured drifter trajectory (c) (Kerdreux et al., 1986).
Trajectoires horizontales et verticales calculées pendant deux jours (la marée a été filtrée en ne reportant qu'un point par cycle de marée) près de la surface (a) et près du fond (b). Trajectoire de flotteur mesurée (c) (Kerdreux et al., 1986).



Tide study

Figure 2 shows the application domains of the two tidal models used in order to provide boundary conditions for the detailed model.

The tide along the French Atlantic coast being mainly semi-diurnal, only the M₂ component has been considered. The boundary conditions for the first model have been roughly extrapolated from the tide measurement points and the general features of tide on the Biscay continental shelf area (Cartwright et al., 1980 ; Vincent and Le Provost, 1988).

The calculated and measured ellipse parameters at points D and R (see Fig. 1) of the M₂ tidal current are listed in the Table. The comparisons show a good agreement at the surface and near the bottom. It may be noted that the changing sign of the semi-minor axis at point D- bottom, indicating a changing rotation from anticlockwise to clockwise at the bed, is well reproduced.

Lagrangian residual currents calculated from the 2-D model results are presented in Figure 3. Except around islands they are very low, especially in the Vilaine bay.

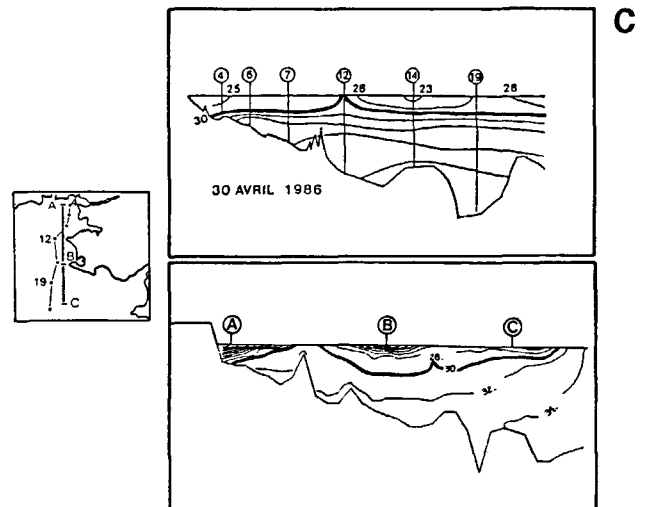
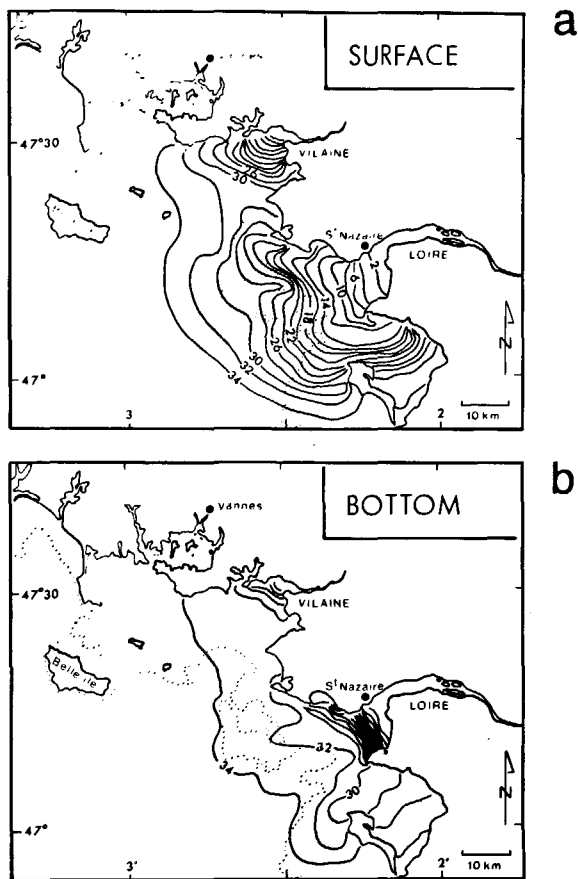


Figure 5

Computed salinities near the surface (a) and the bottom (b) during flood conditions. Comparison between computed and measured salinities on a transect (c).

Salinités calculées près de la surface (a) et du fond (b). Comparaison entre salinités calculées et mesurées sur un profil (c).

Study of wind-induced circulation

Considering the weak tide-induced circulation, wind action was presented as one of the main parameters for water renewal. Figure 4 shows the trajectories of points close to the surface and close to the bottom for a moderate northeasterly wind of 10 m/s. The induced currents are about 5 cm/s and even at shallow depths the inversion of surface and bottom trajectories is visible. Some comparisons done with drifters partially validated the model results. An example is shown in Figure 4 where a drifter moored 9 m below the surface moves against a nearly constant north to east wind; the same phenomenon appears in Figure 4 b from the model results.

Study of Loire and Vilaine water dilution

One purpose of the study was to determine the residence times of waters in the Vilaine bay, where many problematic issues such as high fish mortality and green tides have been observed. From a biological point of view, river inputs are a dominant parameter. The simulation presented in Figure 5 represents the Vilaine and Loire plumes for flood conditions after one week of simulation. It may be noted that those remain at the surface, and that part of the

Loire diluted waters may penetrate the Vilaine bay. These features have been compared (Fig. 5 c) with measurements made during high discharge (Maggi *et al.*, 1987). The agreement is good considering the limitations imposed for the computation (homogeneous initial salinity field, no wind).

CONCLUSION

The system of models presented constitutes a very powerful tool for investigating the main dynamic processes of a coastal zone. The 2-D model, able to include emerging tidal flats with its automatic detailing system and depth discretization, makes it possible to study barotropic phenomena rapidly and with precision. The 3-D model includes all the other parameters, such as wind and density effects.

Although this model is recent, its application to the Mor Bras area demonstrated that it correctly reproduced the prototype (Salomon and Lazure, 1988). Work is continuing on the integration of a more sophisticated turbulence model that will eliminate the empiricism contained in formulations (16) and (17) above. The present first application of the model to a real area proves it to be capable of

reproducing the main dynamic factors in coastal zones. Detailed examination of the modelled results revealed the following main dynamic processes in the Mor Bras zone :
- the tide, which produces the major part of instantaneous currents, has a weak residual effect. Thus, residence times may be expected to be very long during calm wind and dry

conditions, especially in the Vilaine bay;
- wind appears to be the main cause of water renewal, and the induced transports are strongly three-dimensional;
- the simulation of flood conditions has shown that a part of the Loire plume may penetrate the Mor Bras zone, as observed, because of the Coriolis effect.

REFERENCES

- Asselin R.** (1972). Frequency filter for time integrations, *Mon. Weat. Rev.*, **100**, 487-490.
- Blumberg A.F. and G.L. Mellor** (1981). A numerical calculation of the circulation in the Gulf Mexico. *Dynalysis of Princeton*, Princeton, N.J., Rep. 66, 153.
- Burg M.C., Y. Coeffe and A. Warluzel** (1982). Tridimensional numerical model for tidal and wind generated flow. *Proceedings 18th coastal Engineering Conference ASCE, Capetown, South Africa.*, 635-651.
- Cartwright D.E., A.C. Edden, R. Spencer and J.M. Vassie** (1980). The tides of the Northeast Atlantic Ocean. *Phil. Trans. R. Soc., Ser. A.* **298**, 87- 139.
- Gordon R.B.** (1982). Wind-driven circulation in Narragansett bay, *Ph D Thesis, University of Rhode Island.*
- Kerdreux M., M. Merceron, P. Le Hir and M. Breton** (1986). Suivi de flotteurs dans la zone Loire-Vilaine. Rapport IFREMER, DERO-EL 86.30.
- Maggi P., P. Lassus, I. Truquet and L. Soulard** (1987). Facteurs hydro-climatiques et apparitions d'eaux colorées en baie de Vilaine durant l'année 1986. Rapport IFREMER DERO-87.16-MR, 52.
- Munk W.H. and E.R. Anderson** (1948). Notes on the theory of the thermocline. *J. mar. Res.*, **7**, 276-295.
- Peaceman D.W. and H.H. Rachford** (1955). The numerical solution of parabolic and elliptic differential equations, *J. Soc. Ind. applied Math.*, **3**, 1, 28-41.
- Roache J.R.** (1982). *Computational fluid dynamics*. Hermosa Publishers, Albuquerque, New Mexico 87180, USA.
- Salomon J.-C. and P. Lazure** (1988). Étude par modèle mathématique de quelques aspects de la circulation marine entre Quiberon et Noirmoutier. Rapport IFREMER DERO-88.26-EL. 104.
- Takacs L.L.** (1985). A two-step scheme for the advection equation with minimized dissipation and dispersion errors, *Mon. Weath. Rev.*, June 1985, 1050-1065.
- Vincent P. and C. Le Provost** (1988). Semi-diurnal tides in the Northeast Atlantic from a finite element model. *J. geophys. Res.*, **93**, C1, 543-555.